Geomorphology 110 (2009) 162–171

Contents lists available at ScienceDirect

Geomorphology

journal homepage: www.elsevier.com/locate/geomorph

Discriminant analysis of the geomorphic characteristics and stability of landslide dams

Jia-Jyun Dong [a,*], Yu-Hsiang Tung [a], Chien-Chih Chen [b], Jyh-Jong Liao [c], Yii-Wen Pan [c]

[a] Graduate Institute of Applied Geology, National Central University, 300, Jungda Rd., Jungli, Taoyuan, 32001, Taiwan
[b] Graduate Institute of Geophysics, National Central University, 300, Jungda Rd., Jungli, Taoyuan, 32001, Taiwan
[c] Department of Civil Engineering and Hazard Mitigation Research Center, National Chiao Tung University, 1001, University Road, Hsinchu, 30010, Taiwan

ARTICLE INFO

Article history:
Received 12 November 2008
Received in revised form 1 April 2009
Accepted 6 April 2009
Available online 16 April 2009

Keywords:
Landslide dam
Stability
Discriminant analysis
Geomorphic variable

ABSTRACT

Landslides can cause the formation of dams, but these dams often fail soon after lake formation. Thus, rapidly evaluating the stability of a landslide dam is crucial for effective hazard mitigation. This study utilizes discriminant analysis based on a Japanese dataset consisting of 43 well documented landslide dams to determine the significant variables, including log-transformed peak flow (or catchment area), and log-transformed dam height, width and length in hierarchical order, which affect the stability of a landslide dam. The high overall prediction power (88.4% of the 43 training cases are correctly classified) and the high cross-validation accuracy (86%) demonstrate the robustness of the proposed discriminant models PHWL (with variables including log-transformed peak flow, and log-transformed dam height, width and length) and AHWL (with variables including log-transformed catchment area, and log-transformed dam height, width and length). Compared to a previously proposed "*DBI*" index-based graphic approach, the discriminant model AHV – which uses the log-transformed catchment area, dam height, and dam volume as relevant variables – shows better ability to evaluate the stability of landslide dams. Although these discriminant models are established using a Japanese dataset only, the present multivariate statistical approach can be applied for an expanded dataset without any difficulty when more completely documented worldwide landslide-dam data are available.

1. Introduction

The generation and disappearance of landslide-dammed lakes are the results of the complex processes of the earth's surface at the interface between a hillslope and a valley-floor system. Understanding the geomorphic forms and processes involved in the failure of landslide dams is crucial for the purpose of hazard mitigation, as well as the reconstruction of previous events and landscape evolution (Korup, 2002). Regarding catastrophic disasters caused by outburst floods and debris flows, which frequently occur soon after the forming of a natural lake, a rapid assessment of landslide-dam stability is essential (Schuster and Costa, 1986).

Three factors are generally relevant to the occurrence of failure: (1) magnitude and rate of inflow to the dammed reservoir; (2) dimensions of the dam; and (3) material characteristics of the dam (Schuster and Costa, 1986). The material characteristics of landslide dams are difficult to evaluate rapidly if not impossible (Casagli et al., 2003). Currently, the geomorphic approach is widely used to correlate the dam, river, and water-storage characteristics with the landslide dam's stability (Swanson et al., 1986; Costa and Schuster, 1988; Casagli and Ermini, 1999; Ermini and Casagli, 2003; Korup, 2004).

Swanson et al. (1986) suggested that landslide volume and drainage basin area are important factors contributing to the stability of a landslide dam. Casagli and Ermini (1999) proposed that dam height, landslide velocity and the width of the dam valley are significant to the damming process. Ermini and Casagli (2003) utilized the geomorphic index (*DBI*) by combining three important variables (dam height H_d, dam volume V_d, and catchment area A_c) to evaluate the stability of a landslide dam:

$$DBI = log\left(\frac{H_d \cdot A_c}{V_d}\right). \quad (1)$$

A dam with $DBI<2.75$ will be classified as a stable dam, and one with $DBI>3.08$ will be classified as an unstable dam. Incorporating these simplistic geomorphologic analyses, GIS-based modelling can be used to evaluate the potential of river blockage, upstream flooding, and related hazards of outburst floods associated with the probable sudden failure of landslide dams (Clerici and Perego, 2000; Korup, 2005).

The above index-based graphic approach allows for the first-order estimation of landslide-dam stability and the regional comparison of geomorphic boundary conditions necessary for landslide dam formation

* Corresponding author. 300, Jungda Rd., Jungli, Taoyuan, 32001, Taiwan. Tel./fax: +886 3 4224114.
E-mail address: jjdong@geo.ncu.edu.tw (J.-J. Dong).

0169-555X/$ – see front matter © 2009 Elsevier B.V. All rights reserved.
doi:10.1016/j.geomorph.2009.04.004

and failure (Korup, 2004). Nevertheless, there are drawbacks to the index-based graphic approach, such as: (1) subjective selection of the variables; and (2) the relatively low separation performance (25% cases went unclassified; i.e., $2.75 < DBI < 3.08$). These two shortcomings of the index-based graphic approach highlight its simplistic nature. Possible improvements to this approach could be made by considering other variables and by setting up a wider database in order to reach conclusions based on a rigorous statistical analysis (Ermini and Casagli, 2003). Korup (2004) used discriminant analysis to objectively classify the stable and unstable landslide dams with log-transformed geomorphic variables. However, that study was able to only classify 69% of the landslide dams correctly. It is believed that the incompleteness and varying accuracy of the data rendered the classification process insufficient when using a discriminant model (Korup, 2004).

Costa and Schuster (1991) presented the benchmark inventory of 463 occurrences of landslide dams throughout the world. Based on a large set of collected cases, Ermini and Casagli (2003) built an inventory containing more than 500 cases of landslide dams. However, only 84 case histories were documented with complete records of their catchment area (A_c), dam height (H_d), and dam volume (V_d). Korup (2004) compiled 232 landslide dams in New Zealand from the literature, from multi-temporal air photos, and from a 25-m cell size DEM. The geomorphometric parameters of landslide dams, their associated natural reservoirs, and the contributing catchment areas were derived from the GIS platform. The statistical analysis results of these variables are available, but the values of these geomorphic parameters are not listed in the paper.

Tabata et al. (2002) reported a small inventory of 79 Japanese landslide dams (Tabata's inventory; Supplementary Table S1), which have been classified as stable and unstable dams. Japanese landslide dam inventory is utilized in this study, because 43 out of 79 cases have complete records of a total of 16 geomorphic variables which can be statistically analyzed to study the relation between geomorphic variables and landslide dam stability. Based on the data, the main objectives of the present work are: (1) to objectively select the relevant variables from Tabata's inventory and evaluate their contribution to landslide-dam stability (without a failure associated with overtopping, piping, or a slope failure of the dam itself); (2) to test the ability of statistical models for predicting the stability of landslide dams; and (3) to compare the performance of the previously proposed index-based graphic methods with the proposed statistical models. Discriminant analyses are performed using commercial statistical package, SPSS (Statistical Package for the Social Sciences). The relative importance of the relevant variables in the proposed statistical model is evaluated by the standardized canonical discriminant coefficients of the discriminant model. Finally, a discriminant model with the same set of variables considered in the "*DBI*" index-based graphic approach is built using a dataset including 84 landslide-dam cases (Ermini and Casagli, 2003) as the training set. With Tabata's inventory including 37 cases as the target set (none in the training set), we compare the prediction performance of the landslide-dam stability by the discriminant model and by the index-based graphic model (*DBI* index).

2. Landslide-dam data sets

Tabata et al. (2002) studied 79 landslide-dam events that occurred in Japan. The triggering factor, geological and geomorphic characteristics of these landslide dams (Tabata's inventory) and their longevity have been well documented. Fig. 1 illustrates the 16 documented geomorphic variables of these landslide dams. Table 1 lists the definitions of these variables. The variables were mainly derived from historical records. If the variables are not available in the historical records, then aerial photographs, field investigations, and topographical maps (1/25,000) were used (also listed in Table 1) to complete the inventory. It is of note that some of the selected variables – e.g., mean flow, peak flow, lake depth, and lake area – are not time-invariant variables. The time interval used to derive the mean flow is from 1973 to 1982. The peak flow was the record up to 1979. The definitions of depth and area of lakes are not clearly specified by Tabata et al. (2002). It is speculated that the lake depth and its area are the maximum lake depth and area, because most of the lake depth is identical to (or slightly smaller than) the height of the landslide dam (from river bed to overflow point). The variation of the dam's geometry over time is not considered.

The reliability of the data is categorized into: (A) high reliability (the characteristics of the landslide, dam, and lake were well documented or can be accurately determined from topographical maps); (B) medium reliability (the landslide and dam can be accurately located, but the uncertainty of the variables is higher than category A), and (C) low reliability (the landslide and dam cannot be accurately located, and the reliability of the data is low). In Tabata's inventory (79 cases), there were 43 landslide dams (9 stable and 34 unstable ones; the definition of a stable landslide dam is described at the end of this section) for which complete records of all 16 geomorphic variables are available. Among them, 18, 21, and 4 cases are reported with high, medium, and low reliability, respectively. The data (Supplementary Table S1) were statistically analyzed and utilized to build the discriminant models for classifying the stability of landslide dams.

To compare the performance of the prediction between the *DBI* index-based graphic model and the discriminant model, we use the worldwide dataset (with complete records of A_c, H_d, and V_d) of landslide dams collected by Ermini and Casagli (2003). In total, we utilize 84 well

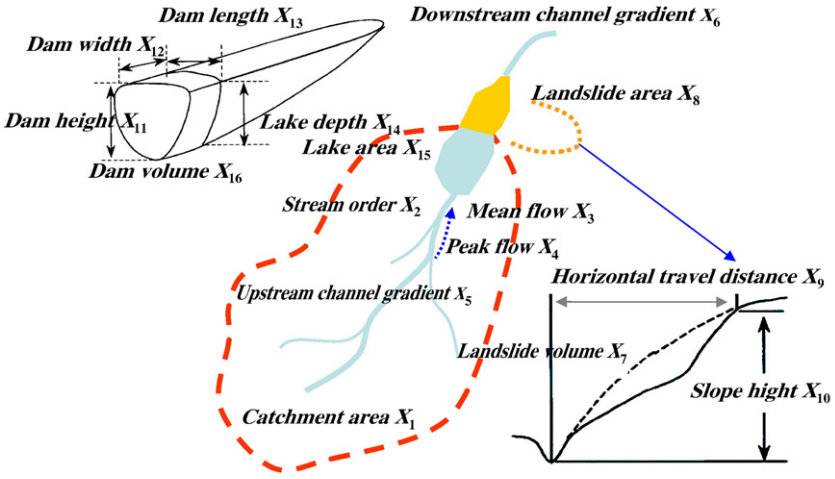

Fig. 1. The 16 variables reported by Tabata et al. (2002). Table 1 lists the definitions of these variables.

Table 1
Geomorphic variables recorded for the Japanese landslide dams (Tabata et al., 2002).

Variables	Definitions (Method used for deriving the variables if historic records are not available)
Catchment area X_1	Catchment area upstream of the stream blockage point (Derived from the topographical maps (1/25 000) using planimeter and digitizer)
Stream order X_2	Stream size at the dammed point in the hierarchy of tributaries (Counted from the topographical maps (1/25 000))
Mean flow X_3	Mean flow of the dammed stream (Estimated from the specific mean flow in the nearby watershed; annual mean flow from 1973 to 1982 recorded by stream gauge station in the nearby watershed was used to calculate specific mean flow)
Peak flow X_4	Peak flow of the dammed stream (Estimated from the specific peak flow of a nearby watershed with similar catchment area of the dammed stream, reported by water resources agency in 1979)
Upstream channel gradient X_5	Mean channel gradient upstream (500–1000 m) of the stream blockage point (Calculated from the topographical maps (1/25,000))
Downstream channel gradient X_6	Mean channel gradient downstream (500–1000 m) of the stream blockage point (Calculated from the topographical maps (1/25,000))
Landslide volume X_7	Volume of landslide materials (Calculated from the landslide area and estimated averaged slide depth)
Landslide area X_8	Area of landslides that contributing material to the landslide dam (Derived from the topographical maps (1/25,000) using planimeter and digitizer)
Horizontal travel distance X_9	Horizontal travel distance between the point of landslide region and river bed (Measured from the topographical maps (1/25,000))
Slope height X_{10}	Vertical distance between the point of landslide region and river bed (Measured from the topographical maps (1/25,000))
Dam height X_{11}	Height of landslide dam, from river bed to overflow point (Measured from the topographical maps (1/25,000))
Dam width X_{12}	Maximum width of landslide dam (along valley) (Measured from the topographical maps (1/25,000))
Dam length X_{13}	Maximum length of landslide dam (across valley) (Measured from the topographical maps (1/25,000))
Lake depth X_{14}	Depth of impounded lake (Measured from the topographical maps (1/25,000))
Lake area X_{15}	Area of impounded lake (Derived from the topographical maps (1/25 000) using planimeter and digitizer)
Dam volume X_{16}	Volume of landslide dam $V_d = 0.5W_dL_dH_d$ (Calculated from width (W_d), length (L_d), and height (H_d); $V_d = 0.5W_dL_dH_d$)

documented case histories (40 stable dams and 44 unstable dams) in Italy, Switzerland, Japan, Canada, the U.S., Guatemala, New Zealand, Papua New Guinea, Peru, Tajikistan, India, and the Kyrgyz Republic (Ermini–Casagli inventory; Supplementary Table S2). Discriminant models are built based on the 84 cases with three log-transformed variables ($\log A_c$, $\log H_d$, and $\log V_d$) which are identical to the ones used for building the DBI index-based graphic models. In Tabata's inventory (79 landslide-dam events), there were 50 cases where the catchment area, dam height and dam volume were completely documented. Among the 50 cases, there are 13 cases already included in the Ermini–Casagli inventory. Therefore, we take the remained 37 Japanese cases for model verification.

Fig. 2 shows the process for building and validating the proposed discriminant model with Tabata and Ermini–Casagli inventories. Forty-three Japanese cases are used to build the statistical models (left part of Fig. 2). The performance of the proposed models is cross-validated and the relative importance of each selected variable is then evaluated. The Ermini–Casagli inventory (84 worldwide cases) is used to build the statistical model with log-transformed variables identical to those used in the *DBI* model (right part of Fig. 2). The performance of the discriminant model and the *DBI* index-based graphic model for predicting the stability of the 37 Japanese cases is now compared.

The definitions of stable and unstable dams are notably crucial for the present study. The term "stable" in relation to landslide dams has to be treated with caution, since it is not time invariant. A present stable landslide dam might be subject to failure by extremely heavy rainfall or a large earthquake some time later. A stable landslide dams, based on the definition of Ermini and Casagli (2003) and Tabata et al. (2002), is a landslide dam which has remained stable over a long period and has not encountered a breach, thus still impounding an existent lake. Korup (2004) defined the "stable landslide dams" in New Zealand as: "The persistence of a landslide dammed lake for over a decade, and usually several decades, has thus been used to assign the stable status". The youngest landslide dams in Ermini–Casagli and Tabata's inventories were formed in 1994 (reported in 2003) and 1984 (reported in 2002), respectively. In other words, the definition of "stable" in relation to landslide dams of the inventory is similar to that adopted by Korup (2004). This definition should be appropriate from the viewpoint of landslide dam hazard mitigation.

3. Methodology

A statistical model for predicting slope instability can be built on the assumption that the factors which cause landslides in a region are the same as those which will again fail in the future (Carrara et al., 2008). In this study we try to classify the landslide dams into two groups on the basis of the discriminant analysis of a set of variables: (1) the stable group and (2) the unstable group. The methodology adopted in this study is shown in a flow chart (Fig. 2) and is described briefly as follows.

3.1. Discriminant analysis

3.1.1. Categorizing the dataset

The purpose of discriminant analysis is to find a linear equation (discriminant function) to separate two or more groups of objects with respect to several variables simultaneously (Klecka, 1980). In this study we categorize the data for landslide dams into stable and unstable groups. The discriminant function has the form:

$$D = b_0 + b_1x_1 + b_2x_2 + \ldots + b_nx_n, \quad (2)$$

where D is the discriminant score; x_i ($i = 1, 2, \ldots, n$) is the independent variable; b_i ($i = 0, 1, 2, \ldots, n$) is the unstandardized canonical coefficient of the discriminant function for the i-th variable; and n is the number of independent variables. If a dam with variable x_i results in $D>0$, then it is categorized into the stable group; otherwise, it will be placed into the unstable group. The coefficients of the linear discriminant function can be determined by solving the general eigenvalue problem. Several multivariate statistics texts (e.g., Cooley and Lohnes, 1971; Klecka, 1980; Davis, 2002) cover the mathematical derivation of the coefficients.

Two basic assumptions on the statistical properties of the causative factors in a discriminant function are: (1) each group is drawn from a population which has a multivariate normal distribution; and (2) no variable may be a linear combination of other variables (Klecka, 1980). Therefore, checking the normality of the dataset and the interdependence of the previously selected 16 variables is required for statistical susceptibility modelling.

3.1.2. Normality test of the dataset and dependency of the variables

The descriptive statistics related to the 16 variables for landslide dams are first demonstrated. We test the variables for the normality of distribution using the Kolmogorov–Smirnov (K–S) test at a 5% confidence level (α). When the distribution of the sample is not symmetrical but positively skewed, this distribution can be transformed with logarithms to obtain a normal distribution (Baeza and Corominas, 2001).

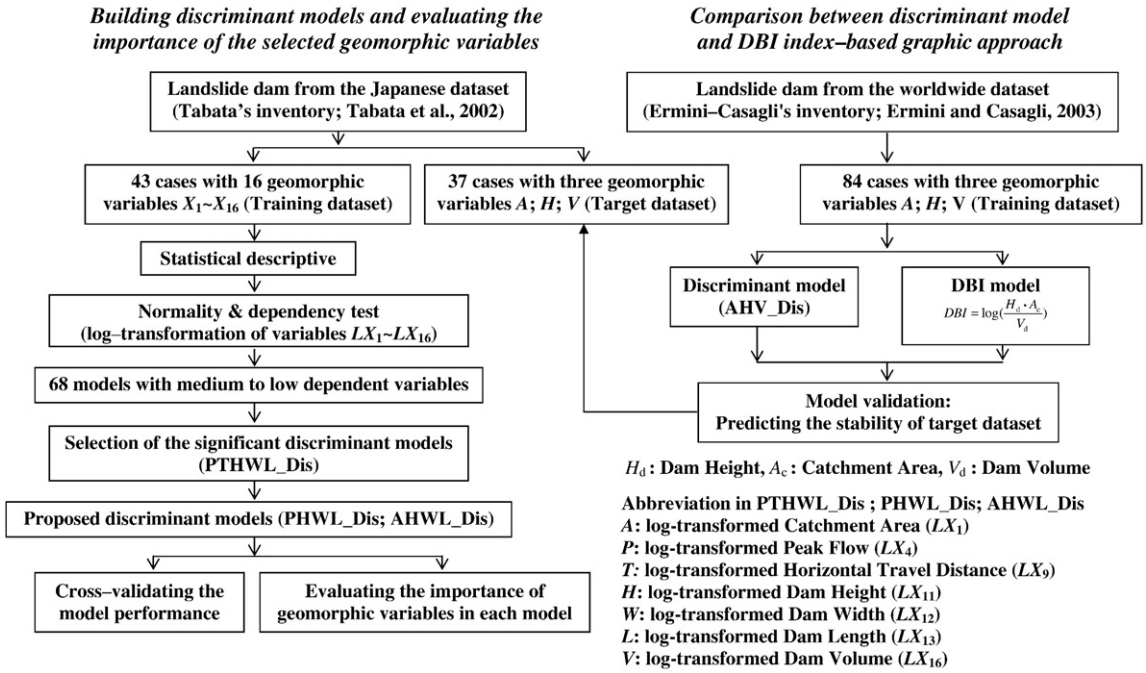

Fig. 2. The process and methodology used in building the discriminant models for predicting the landslide-dam stability (left) and the comparison between the proposed discriminant model and the *DBI* model (right).

The performance of a linear discriminant function is likely to be poor when dealing with populations characterized by a strong correlation between variables (Dillon and Goldstein, 1986). Consequently, models which are composed of independent variables are preferable. The dependency of variables can be evaluated using the correlation coefficient. Klecka (1980) provided the method and example for deriving a correlation coefficients matrix of a set of variables. The proper selection of variables to minimize the correlation coefficients between variables is important. Korup (2004) suggested that the absolute value of the correlation coefficient 0.5–0.7 represents a moderate correlation between two variables. In this study an absolute value of the correlation coefficient larger than 0.6 is thought to represent a high correlation between two variables. Accordingly, all models composed of log-transformed variables with low to moderate correlations are identified.

3.1.3. Model selection

Based on the derived matrix of correlation coefficients, one can determine the models with all possible combinations of low to moderate correlation variables (those with absolute value of the correlation coefficient<0.6). One challenge lies in: how does one find the most discriminant model from all of the models with low to moderate correlation variables? Wilks' lambda is frequently used to test whether there are differences between the means of identified groups for a combination of dependent variables selected by a discriminant model (Klecka, 1980). Because Wilks' lambda is a kind of inverse measure, values of Wilks' lambda which are near zero denote high discrimination between groups. Generally, if the significance of a discriminant model is less than 0.05, then this represents sufficient discriminatory power. We use the significance level of Wilks' lambda to screen out the suitable models among the identified models with low to moderate correlation variables.

3.1.4. Relative importance of the variables influencing the landslide-dam stability

After suitable models with relevant log-transformed variables are identified, the relative importance of each variable in the prediction model can be evaluated using the standardized canonical discriminant

Table 2
Descriptive statistics of geomorphic variables for Japan's landslide dams (n = 43).

Geomorphic variables	Minimum	Maximum	Mean	S.E.	Standard deviation	Median	Skewness	Kurtosis
Catchment area (m^2) X_1	0.19×10^6	2630×10^6	208.46×10^6	65.79×10^6	431.42×10^6	60×10^6	4.51	24.23
Stream order X_2	2	8	5.44	0.20	1.32	6	−0.758	0.71
Mean flow (cms) X_3	1	100	17.05	3.92	25.73	5	1.89	2.61
Peak flow(cms) X_4	1	6 900	1 450.49	285.53	1 872.36	750	1.62	1.63
Upstream channel gradient X_5	0.00222	0.33	0.04	0.0092	0.06	0.0143	3.23	12.98
Downstream channel gradient X_6	0.00213	0.25	0.04	0.0085	0.06	0.0200	2.86	8.65
Landslide volume (m^3) X_7	0.009×10^6	130×10^6	14.24×10^6	4.41×10^6	28.92×10^6	3.7×10^6	3.14	9.71
Landslide area (m^2) X_8	0.003×10^6	2.3×10^6	0.33×10^6	0.07×10^6	0.48×10^6	0.16×10^6	2.77	7.98
Horizontal travel distance (m) X_9	130	6 000	1 153.26	181.45	1 189.88	830	2.71	8.22
Slope height (m) X_{10}	25	1 000	408.49	35.48	232.63	370	0.71	−0.08
Dam height (m) X_{11}	5	190	50.81	5.93	38.89	45	1.36	2.75
Dam width (m) X_{12}	90	3 300	420.47	75.20	493.09	300	4.97	28.82
Dam length (m) X_{13}	50	700	294.60	29.17	191.30	250	0.75	−0.64
Lake depth (m) X_{14}	4.50	190	47.69	5.79	37.97	38	1.57	3.69
Lake area (m^2) X_{15}	0.002×10^6	18×10^6	1.06×10^6	0.43×10^6	2.84×10^6	0.28×10^6	5.36	31.48
Dam volume (m^3) X_{16}	0.0045×10^6	26×10^6	3.60×10^6	0.9×10^6	5.92×10^6	1.2×10^6	2.54	6.06

Table 3
Kolmogorov–Smirnov (K–S) test for data normality.

Original geomorphic variables	Confidence level α	Log-transformed variables	Confidence level α
X_1 (catchment area)	0.000	LX_1 (log X_1)	0.587
X_2 (stream order)	0.028	LX_2 (log X_2)	0.019
X_3 (mean flow)	0.000	LX_3 (log X_3)	0.388
X_4 (peak flow)	0.021	LX_4 (log X_4)	0.479
X_5 (upstream channel gradient)	0.005	LX_5 (log X_5)	0.353
X_6 (downstream channel gradient)	0.003	LX_6 (log X_6)	0.898
X_7 (landslide volume)	0.000	LX_7 (log X_7)	0.377
X_8 (landslide area)	0.001	LX_8 (log X_8)	0.741
X_9 (horizontal travel distance)	0.028	LX_9 (log X_9)	0.957
X_{10} (slope height)	0.493	LX_{10} (log X_{10})	0.550
X_{11} (dam height)	0.572	LX_{11} (log X_{11})	0.515
X_{12} (dam width)	0.009	LX_{12} (log X_{12})	0.785
X_{13} (dam length)	0.180	LX_{13} (log X_{13})	0.584
X_{14} (lake depth)	0.485	LX_{14} (log X_{14})	0.531
X_{15} (lake area)	0.000	LX_{15} (log X_{15})	0.864
X_{16} (dam volume)	0.000	LX_{16} (log X_{16})	0.847

coefficient (*SCDC*). The relative importance of the log-transformed variable for group characterization grows with an increasing *SCDC*. The formulation for deriving *SCDC* from the unstandardized canonical coefficients can be found in Klecka (1980).

3.2. Evaluation of the performance of a predictive model

A confusion matrix is often used to demonstrate the performance of a prediction model. Once a characterizing threshold has been adopted, the binary predictions can be compared with the samples, allowing for the construction of the confusion matrix. The confusion matrix shows the portion of correctly and incorrectly predicted observations, for both stable and unstable landslide dams. We can then compare the model's efficiency, which is evaluated by the proportion of correctly classified observations, to different discriminant models with log-transformed variables.

Cross-validation is frequently used to test the reliability and robustness of a statistical model (Carrara et al., 2008). We split the dataset (43 cases) randomly into: (1) the training set (17 unstable and five stable); and (2) the target set (17 unstable and four stable). We next evaluate the predictive success of the model, built on the training set, by using the target set. The proportion of correctly classified observations is calculated to illustrate the prediction ability of the proposed statistical models.

Drawbacks exist when evaluating the predictive model with a confusion matrix, as they are highly dependent on the proportion of positive and negative groups in the sample (Begueria, 2006). Alternatively, the prediction performance of a predictive model can be evaluated via a Relative Operating Characteristic (ROC) diagram, which has been widely used to measure prediction potential of landslide susceptibility models (e.g., Chung and Fabbri, 2003; Chang et al., 2007; Chen et al., 2007; Carrara et al., 2008; Lee et al., 2008a,b). In the ROC graph the false alarm rate (*FAR*) is plotted on the horizontal axis and the hit rate (*HR*) on the vertical axis. *HR* is the fraction of positive occurrences of dam failure that have been correctly predicted, while *FAR* is the fraction of incorrectly predicted cases that did not occur (Swets, 1988). A larger area under the ROC Curve (*AUC*) indicates better model prediction (*AUC* index ranges from 0.5 for models with no predictive capability to 1.0 for models with perfect predictive power). These discriminant analyses are carried out using the commercial statistical package, SPSS (Statistical Package for the Social Sciences).

4. Results

4.1. Descriptive statistics and normality test of variables

Table 2 lists the descriptive statistics of 16 variables (X_1–X_{16}). Basically, the catchment area upstream of a blockage point in the Japanese dataset (0.19–2 630 km^2) falls within the same order as the New Zealand landslide dams (0.2–4492 km^2) reported by Korup (2004). However, the mean dam volume (3.6 Mm^3) of the studied dataset is about one order smaller than that for the worldwide dataset (rainfall triggered: 31.1 Mm^3; earthquake triggered: 80.2 Mm^3) as reported by Ermini and Casagli (2003) and about two orders smaller than that of Korup's dataset (302.6 Mm^3). The statistics results indicate the large scatter nature of the geomorphic variables of landslide dams. It is of note that the following statistical approach should be verified carefully and can only be applied to those cases with similar characteristics.

The confidence levels of the Kolmogorov–Smirnov (K–S) test for the 16 variables are calculated and listed in Table 3. From the second column of Table 3, it can be seen that most of the variables, where $\alpha<0.05$, are not normal-distribution variables. Korup (2004) indicated that the variables of landslide dams are log-normal distribution variables, because the skewness and kurtosis of the variables are high. After the log-transformation of the selected variables (denoted as LX_1–LX_{16}) is taken, the confidence level of the K–S test $\alpha>0.05$ implies that the geomorphic variables are distributed in the log-normal manner except the stream order (LX_2). However, LX_2 is ruled out in the following analysis since the catchment area is a similar indicator of stream order.

4.2. Correlation coefficients of the log-transformed geomorphic variables

The selected log-transformed variables are categorized as Catchment (C), landslide (L), and landslide dam (lake) (D) groups (Table 4).

Table 4
Matrix showing the correlation coefficients of logtransformed geomorphic variables.

		Catchment (*C*)					Landslide (*L*)				Dam and lake (*D*)					
		LX_1	LX_3	LX_4	LX_5	LX_6	LX_7	LX_8	LX_9	LX_{10}	LX_{11}	LX_{12}	LX_{13}	LX_{14}	LX_{15}	LX_{16}
C	LX_1	1.000	0.866	0.926	−0.773	−0.726	*0.362*	*0.383*	*0.481*	*0.518*	*−0.079*	*0.457*	*0.238*	*−0.103*	0.640	*0.195*
	LX_3		1.000	0.780	−0.716	−0.797	*0.186*	*0.206*	*0.291*	*0.266*	*−0.187*	*0.337*	*−0.034*	*−0.230*	*0.435*	*−0.032*
	LX_4			1.000	−0.759	−0.706	*0.395*	*0.410*	*0.467*	0.607	*−0.101*	*0.386*	*0.180*	*−0.132*	*0.524*	*0.159*
	LX_5				1.000	0.751	*0.027*	*−0.059*	*−0.193*	*−0.229*	*0.354*	*−0.118*	*−0.009*	*0.382*	*−0.332*	*0.189*
	LX_6					1.000	*0.013*	*−0.010*	*−0.070*	*−0.047*	*0.307*	*−0.187*	*0.128*	*0.316*	*−0.278*	*0.199*
L	LX_7						1.000	0.818	0.671	0.653	*0.338*	0.655	*0.559*	*0.347*	*0.587*	0.660
	LX_8							1.000	0.661	0.662	*0.235*	0.612	*0.437*	*0.243*	*0.517*	*0.566*
	LX_9								1.000	0.850	*−0.001*	*0.330*	*0.342*	*0.031*	*0.460*	*0.295*
	LX_{10}									1.000	*0.060*	*0.365*	*0.319*	*0.061*	*0.412*	*0.331*
D	LX_{11}										1.000	*0.328*	*0.535*	0.982	*0.489*	0.730
	LX_{12}											1.000	*0.465*	*0.315*	0.617	0.693
	LX_{13}												1.000	*0.555*	0.752	0.817
	LX_{14}													1.000	*0.490*	0.728
	LX_{15}														1.000	0.724
	LX_{16}															1.000

Values in Italic show correlation coefficients<0.6.

Table 5
Wilks' Lambda significance level of 68 models with combinations of low to moderate correlation variables (log-transformed variables).

Number	Models with different variable combinations	Wilks' Lambda significance level	Number	Models with different variable combinations	Wilks' Lambda significance level
1	LX_1. LX_7. LX_{11}. LX_{13}	0.002	35	LX_4. LX_9. LX_{12}. LX_{13}. LX_{14}[a]	1.96×10^{-4}
2	LX_1. LX_7. LX_{13}. LX_{14}	0.001	36	LX_4. LX_9. LX_{14}. LX_{15}	0.001
3	LX_1. LX_8. LX_{11}. LX_{13}	0.002	37	LX_5. LX_7. LX_{11}. LX_{13}	0.004
4	LX_1. LX_8. LX_{13}. LX_{14}	0.001	38	LX_5. LX_7. LX_{11}. LX_{15}	0.017
5	LX_1. LX_9. LX_{11}. LX_{12}. LX_{13}	0.001	39	LX_5. LX_7. LX_{13}. LX_{14}	0.002
6	LX_1. LX_9. LX_{12}. LX_{13}. LX_{14}	4.43×10^{-4}	40	LX_5. LX_7. LX_{14}. LX_{15}	0.013
7	LX_1. LX_{10}. LX_{11}. LX_{12}. LX_{13}	0.001	41	LX_5. LX_8. LX_{11}. LX_{13}	0.003
8	LX_1. LX_{10}. LX_{12}. LX_{13}. LX_{14}	4.55×10^{-4}	42	LX_5. LX_8. LX_{11}. LX_{15}	0.013
9	LX_3. LX_7. LX_{11}. LX_{13}	0.006	43	LX_5. LX_8. LX_{13}. LX_{14}	0.002
10	LX_3. LX_7. LX_{11}. LX_{15}	0.010	44	LX_5. LX_8. LX_{14}. LX_{15}	0.010
11	LX_3. LX_7. LX_{13}. LX_{14}	0.004	45	LX_5. LX_9. LX_{11}. LX_{12}. LX_{13}	0.006
12	LX_3. LX_7. LX_{14}. LX_{15}	0.007	46	LX_5. LX_9. LX_{11}. LX_{15}	0.018
13	LX_3. LX_8. LX_{11}. LX_{13}	0.005	47	LX_5. LX_9. LX_{12}. LX_{13}. LX_{14}	0.004
14	LX_3. LX_8. LX_{11}. LX_{15}	0.009	48	LX_5. LX_9. LX_{14}. LX_{15}	0.014
15	LX_3. LX_8. LX_{13}. LX_{14}	0.003	49	LX_5. LX_{10}. LX_{11}. LX_{12}. LX_{13}	0.003
16	LX_3. LX_8. LX_{14}. LX_{15}	0.006	50	LX_5. LX_{10}. LX_{11}. LX_{15}	0.013
17	LX_3. LX_9. LX_{11}. LX_{12}. LX_{13}	0.003	51	LX_5. LX_{10}. LX_{12}. LX_{13}. LX_{14}	0.002
18	LX_3. LX_9. LX_{11}. LX_{15}	0.010	52	LX_5. LX_{10}. LX_{14}. LX_{15}	0.010
19	LX_3. LX_9. LX_{12}. LX_{13}. LX_{14}	0.002	53	LX_6. LX_7. LX_{11}. LX_{13}	0.002
20	LX_3. LX_9. LX_{14}. LX_{15}	0.007	54	LX_6. LX_7. LX_{11}. LX_{15}	0.003
21	LX_3. LX_{10}. LX_{11}. LX_{12}. LX_{13}	0.001	55	LX_6. LX_7. LX_{13}. LX_{14}	0.002
22	LX_3. LX_{10}. LX_{11}. LX_{15}	0.008	56	LX_6. LX_7. LX_{14}. LX_{15}	0.003
23	LX_3. LX_{10}. LX_{12}. LX_{13}. LX_{14}	0.001	57	LX_6. LX_8. LX_{11}. LX_{13}	0.001
24	LX_3. LX_{10}. LX_{14}. LX_{15}	0.005	58	LX_6. LX_8. LX_{11}. LX_{15}	0.002
25	LX_4. LX_7. LX_{11}. LX_{13}	0.001	59	LX_6. LX_8. LX_{13}. LX_{14}	0.001
26	LX_4. LX_7. LX_{11}. LX_{15}	0.001	60	LX_6. LX_8. LX_{14}. LX_{15}	0.002
27	LX_4. LX_7. LX_{13}. LX_{14}	3.86×10^{-4}	61	LX_6. LX_9. LX_{11}. LX_{12}. LX_{13}	0.001
28	LX_4. LX_7. LX_{14}. LX_{15}	0.001	62	LX_6. LX_9. LX_{11}. LX_{15}	0.003
29	LX_4. LX_8. LX_{11}. LX_{13}	0.001	63	LX_6. LX_9. LX_{12}. LX_{13}. LX_{14}	0.001
30	LX_4. LX_8. LX_{11}. LX_{15}	0.002	64	LX_6. LX_9. LX_{14}. LX_{15}	0.003
31	LX_4. LX_8. LX_{13}. LX_{14}	4.44×10^{-4}	65	LX_6. LX_{10}. LX_{11}. LX_{12}. LX_{13}[d]	3.20×10^{-4}
32	LX_4. LX_8. LX_{14}. LX_{15}	0.001	66	LX_6. LX_{10}. LX_{11}. LX_{15}	0.001
33	LX_4. LX_9. LX_{11}. LX_{12}. LX_{13}[c]	3.09×10^{-4}	67	LX_6. LX_{10}. LX_{12}. LX_{13}. LX_{14}[b]	2.98×10^{-4}
34	LX_4. LX_9. LX_{11}. LX_{15}	0.001	68	LX_6. LX_{10}. LX_{14}. LX_{15}	0.001

[a–d]The most significant models with the lowest significant level.

Table 6
Overall prediction power and the cross-validation accuracy of the four most significant discriminant models.

Model number in Table 5 (variables[a])	Wilks' Lambda significance level	Percentage of landslide dams correctly classified	
		Whole dataset (43 cases)	Cross validation
33 (LX_4, LX_9, LX_{11}, LX_{12}, LX_{13})	3.09×10^{-4}	88.4%	83.7%
35 (LX_4, LX_9, LX_{12}, LX_{13}, LX_{14})	1.96×10^{-4}	88.4%	83.7%
65 (LX_6, LX_{10}, LX_{11}, LX_{12}, LX_{13})	3.20×10^{-4}	88.4%	81.4%
67 (LX_6, LX_{10}, LX_{12}, LX_{13}, LX_{14})	2.98×10^{-4}	86.0%	81.4%

[a] LX_4 (log-transformed peak flow), LX_6 (log-transformed downstream channel gradient), LX_9 (log-transformed horizontal travel distance), LX_{10} (log-transformed slope height), LX_{11} (log-transformed dam height), LX_{12} (log-transformed dam width), LX_{13} (log-transformed dam length), and LX_{14} (log-transformed lake depth).

The within-group correlation between the catchment group and the landslide group is relatively high. Utilizing the correlation coefficients matrix, we can determine the models with all possible combinations of low to moderate correlation variables (absolute value of the correlation coefficient<0.6, Italic in Table 4). Accordingly, 68 models (Table 5) are identified with different variable combinations, all of which are absolute value correlation coefficients between two variables less than 0.6. Notably, the log-transformed dam volume LX_{16} does not appear in Table 5 since in the Japanese cases the dam volume was derived from dam geometry.

4.3. Identifying significant models

The suitability of the 68 statistic models for predicting the stability of landslide dams using relatively independent log-transformed variables can be objectively indicated by the Wilks' Lambda significance level. Table 5 shows the Wilks' Lambda significance level for the 68 models obtained with different variable combinations. It should be noted that each model can be further categorized into sub-models with the combination of the selected log-transformed variables. All Wilks' Lambda significance levels are less than 0.05, implying all 68 models are significant.

The most significant predictive models with the lowest Wilks' Lambda significance level are models 33, 35, 65, and 67. Table 6 shows the overall prediction power (percentage of landslide dams correctly classified) and the cross-validation accuracy of these models. Models 33 and 35 are superior to models 65 and 67 either from the overall prediction power or cross-validation accuracy. The selected variables for model number 33 (LX_4, LX_9, LX_{11}, LX_{12}, LX_{13}) are almost identical to those of model number 35 (LX_4, LX_9, LX_{12}, LX_{13}, LX_{14}), except that log-transformed dam height (LX_{11}) is selected instead of log-transformed lake depth (LX_{14}). Since lake depth is apt to vary, a combination of log-transformed peak flow, horizontal travel distance, dam height, dam

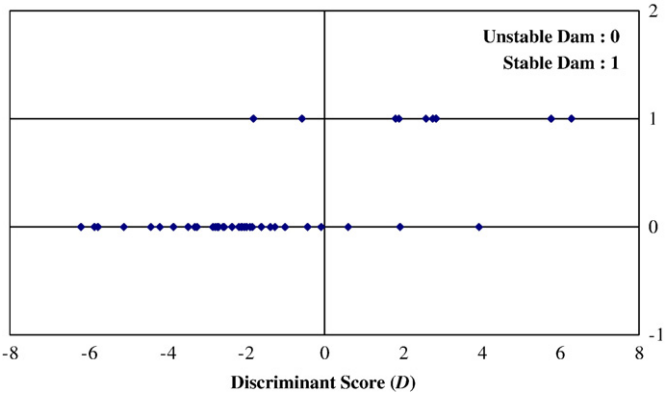

Fig. 3. Discriminant score distribution ($D>0$ stable, $D<0$ unstable) of model PTHWL_Dis for the stability of 43 landslide dams.

width, and dam length (LX_4, LX_9, LX_{11}, LX_{12}, LX_{13}) is considered as the most suitable model (model number 33) and will be analyzed and discussed further. The definitions of the variables in the selected model 33 are indicated in Table 1 and illustrated in Fig. 1.

4.4. Discriminant models

4.4.1. Model PTHWL

The statistical model containing parameters LX_4, LX_9, LX_{11}, LX_{12}, and LX_{13} (log-transformed Peak flow, horizontal Travel distance, dam Height, dam Width, and dam Length) is referred to as the PTHWL model (model number 33). A discriminant model (PTHWL_Dis) is built on the basis of 34 unstable dams and nine stable dams as follows:

$$D = -3.06LX_4 + 0.74LX_9 - 4.46LX_{11} + 4.08LX_{12} + 2.10LX_{13} - 3.65 \quad (3)$$

If a dam with variables x_i results in $D>0$, then it is moved into the stable group; otherwise, it will be moved into the unstable group. Fig. 3 shows the classification results for the discriminant model (PTHWL_Dis). It is observed that seven out of the nine stable landslide dams and 31 out of the 34 unstable landslide dams are correctively classified by the discriminant model. The overall prediction power (percentage of landslide dams correctly classified) is 88.4%. The cross-validation accuracy of model PTHWL_Dis is 83.7%.

Table 7 *SCDC* of the five variables. The LX_4 (log-transformed peak flow) has the largest *SCDC*, which indicates that peak flow plays the most important role in the discriminate stability of landslide dams. If a variable has a negative *SCDC*, then it represents a negative effect on the stability of a landslide dam. Accordingly, the stability of landslide dams decreases as the log-transformed peak flow (LX_4) and/or dam height (LX_{11}) increases. Among the five variables selected, *SCDC* of the log-transformed horizontal travel distance (LX_9) is the lowest, which means that LX_9 is, in this case, a relatively unimportant variable influencing the stability of landslide dams.

4.4.2. Model PHWL

Since the importance of LX_9 on the predictability of the model is insignificant, another model is proposed. The statistical model containing parameters LX_4, LX_{11}, LX_{12}, and LX_{13} (log-transformed Peak flow, dam Height, dam Width, and dam Length), which is referred to as the PHWL model, can be derived using discriminant analysis (PHWL_Dis):

$$D = -2.94LX_4 - 4.58LX_{11} + 4.17LX_{12} + 2.39LX_{13} - 2.52 \quad (4)$$

The overall prediction power of the models is 88.4%, which is identical to that of PTHWL_Dis. The cross-validation accuracy of model PHWL_Dis is 86.0%, which is even higher than that of PTHWL_Dis. This indicates that the statistical model PHWL_Dis is more robust when the variable of log-transformed horizontal travel distance is eliminated. As compared in Table 6, model PHWL_Dis is more significant (significance level 1.09×10^{-4}) than models 33, 35, 65, and 67. Regarding the relative importance of the relevant variables in the models, log-transformed peak flow (LX_4) is still the most significant variable influencing landslide-dam stability, and log-transformed dam height (LX_{11}), dam width (LX_{12}), and dam length (LX_{13}), in sequential order, are less significant, based on the SCDC (Table 8).

Table 7
Standardized canonical discriminant coefficient (*SCDC*) of five log-transformed variables (PTHWL_Dis model).

Variables (log-transformed)	*SCDC*
Peak flow (LX_4)	−1.083
Horizontal travel distance (LX_9)	0.122
Dam height (LX_{11})	−0.763
Dam width (LX_{12})	0.562
Dam length (LX_{13})	0.291

Table 8
Standardized canonical discriminant coefficient (*SCDC*) of four log-transformed variables (PHWL_Dis model).

Variables (log-transformed)	*SCDC*
Peak flow (LX_4)	−1.045
Dam height (LX_{11})	−0.788
Dam width (LX_{12})	0.577
Dam length (LX_{13})	0.332

4.4.3. Model AHWL

Due to the fact that there is often limited time for hazard mitigation after the formation of a landslide dam, a rapid evaluation of the stability of that dam is required. An empirical statistical model such as Eq. (4) could provide a first-order estimation of the landslide dam's stability. However, peak flow is not always available, because only a few dammed rivers in mountainous areas are accurately gauged.

It is well recognized that peak flow correlates well with the catchment area (McCuen, 1998). Using the datasets of Tabata et al. (2002), a linear equation in log–log scale (least squares fitting) can be derived (Fig. 4):

$$P = 16.12A_c^{0.88} \quad (5)$$

where P is the peak flow (m^3/s) and A_c (m^2) is the catchment area. We now propose a replacement of the log-transformed peak flow by log-transformed catchment area in the discriminant model.

The statistical model containing parameters LX_1, LX_{11}, LX_{12}, and LX_{13} (log-transformed catchment Area, dam Height, dam Width, and dam Length), which is referred to as the *AHWL* model, is a sub-model of model 5 shown in Table 5, only excluding the parameter of the log-transformed horizontal travel distance (LX_9; insignificant variable as demonstrated previously). After discriminant analysis, we derive the following equation (AHWL_Dis):

$$D = -2.62LX_1 - 4.67LX_{11} + 4.57LX_{12} + 2.67LX_{13} + 8.26 \quad (6)$$

The significance level of this model is 2.31×10^{-4}, indicating that the model is significant for classifying the stability of landslide dams given the relevant variables. The overall prediction power and cross-validation accuracy of AHWL_Dis are 88.4% and 86.0%, respectively, which are identical to those of model PHWL_Dis.

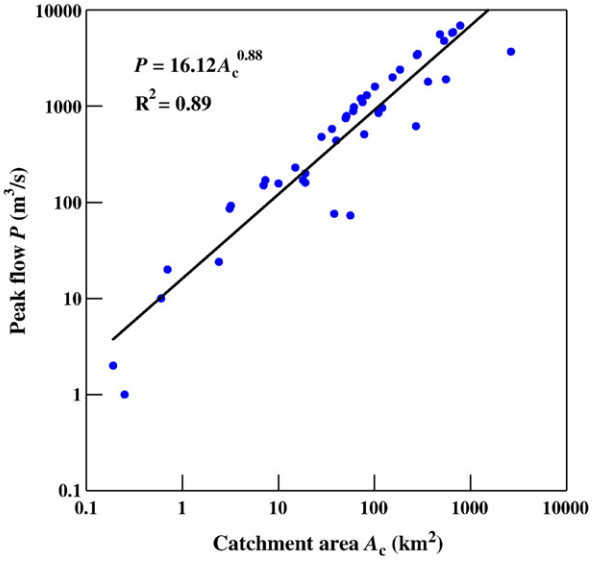

Fig. 4. The relation between peak flow (P) and catchment area (A_c) based on the dataset of 59 landslide dams in Tabata et al. (2002).

Since the log-transformed peak flow (LX_4) is the most significant variable in the PHWL_Dis model, the substituted log-transformed catchment area (LX_1) is not surprisingly still evaluated as being the most influential variable, according to standardized canonical discriminant coefficient (Table 9). The rest of the variables have a significance ranking identical to those obtained from the predictive model PHWL_Dis.

5. Discussion

5.1. Factors dominating the instability of landslide dams

Three failure mechanisms of landslide dams are identified: overtopping, piping, and slope failure (Schuster and Costa, 1986; Swanson et al., 1986). Of these, overtopping is the most important one (Schuster and Costa, 1986). Therefore, it is logical to select the peak flow or catchment area of a blocked stream as the most important variable contributing to the stability of landslide dams. This is why the catchment area is frequently incorporated into the index-based graphic approach to classify the stability of a landslide dam (Impoundment index, dimensionless impoundment index, and Basin Index proposed by Casagli and Ermini, 1999; Ermini and Casagli, 2003; Korup, 2004, respectively).

The volume of a landslide dam, which reflects a "resisting" force as opposed to the catchment area as a "removing" force (Korup, 2004), plays an important positive role in the stability of landslide dams. The dam height, which might correlate with the volume of a landslide dam, has a negative effect on the stability of a landslide dam, because the higher the dam is, the larger the seepage driving force. The dimensionless impoundment index *DBI* fully accounts for the above combined effects of stream flow and dam geometry.

Three points need to be highlighted in our study. First, discriminant analysis is a rigorous and relatively objective procedure for finding the four most relevant variables from the 16 variables listed in Table 1, although the discriminant analysis yields a similar set of relevant variables as the index-based graphic approach. Secondly, the graphically derived critical thresholds of the dimensionless impoundment index assume the log-transformed volume and height of a landslide dam as the relevant variables. However, these two log-transformed variables are not independent variables (see Table 4; correlation coefficient = 0.730 represents a high correlation between LX_{11} and LX_{16}), although there is no inherent need for independence of variables when using dimensionless impoundment index.

Very often, the dam volume is derived from the geometry of the dam (i.e., height, width, and length). In our discriminant models PHWL and AHWL, dam geometry, including log-transformed dam height, width, and, length are treated as independent variables (correlation coefficient = 0.328, 0.465, and 0.535 represents a corresponding low to medium correlation between LX_{11} and LX_{12}, LX_{12} and LX_{13}, and LX_{11} and LX_{13}). Last but not the least, the index-based graphic approach provides little information about the relative importance of each selected variable as it pertains to the stability of a landslide dam.

Aside from the most significant variables (log-transformed peak flow or catchment area), discriminant analysis successfully demonstrates that the log-transformed dam height (LX_{11}) has a stronger impact on dam stability than the other two geometrical variables (LX_{12} and LX_{13}) and it makes a negative contribution to the stability of a landslide dam. On the other hand, both the log-transformed dam width (LX_{12}) and length (LX_{13}) have positive effects on a dam's stability. It also appears that the log-transformed dam width along the channel always has a larger contribution to dam stability than the dam length from their *SCDC*.

Table 9
Standardized canonical discriminant coefficient (*SCDC*) of four log-transformed variables (AHWL_Dis model).

Variables (log-transformed)	*SCDC*
Catchment area (LX_1)	−1.085
Dam height (LX_{11})	−0.842
Dam width (LX_{12})	0.663
Dam length (LX_{13})	0.390

Table 10
Confusion matrix of the discriminant models.

Model	Actual groups	Number of landslide dams	Predicted group membership	
			Group 1 (stable)	Group 2 (unstable)
PTHWL_Dis	Group 1 (stable)	9	77.8%	22.2%
	Group 2 (unstable)	34	8.8%	91.2%
	Percentage of landslide dams correctly classified: 88.4 (whole dataset; 43 cases) 83.7 (cross-validation)			
PHWL_Dis[a]	Group 1 (stable)	9	77.8%	22.2%
	Group 2 (unstable)	34	8.8%	91.2%
	Percentage of landslide dams correctly classified: 88.4 (Whole dataset; 43 cases) 86.0 (cross-validation)			
AHWL_Dis[b]	Group 1 (stable)	9	77.8%	22.2%
	Group 2 (unstable)	34	8.8%	91.2%
	Percentage of landslide dams correctly classified: 88.4 (Whole dataset; 43 cases) 86.0 (cross-validation)			

[a] Proposed discriminant model (Eq. (4)).
[b] Proposed discriminant model (Eq. (6)).

5.2. Quality of the discriminant models

In this study we adopt the widely-used cross-validation technique to assess the quality of all of the proposed discriminant models. Some arguments may arise since the models are not validated using a dataset independent of the one used for training. Carrara et al. (2008) discussed the difficulty of validating landslide susceptibility models with datasets that are separated from the training set either spatially or temporally. More cases with complete records of different relevant variables are required to eliminate the drawback of multivariate analyses as stated by Korup (2004). He mentioned "…incompleteness and varying accuracy of data render the use of multivariate analyses for meaningful differentiation, classification, or stability prediction

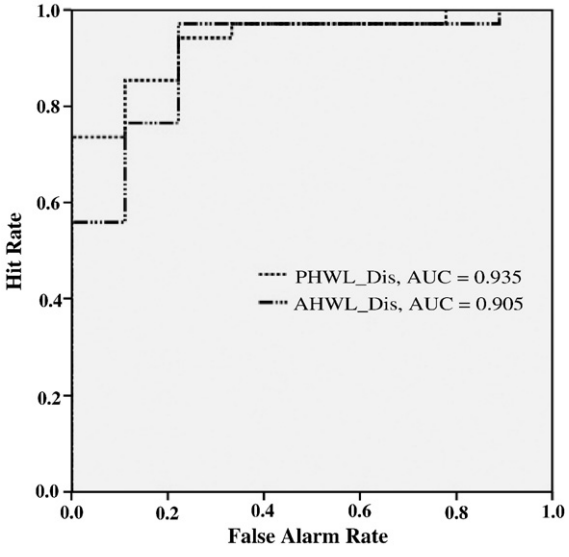

Fig. 5. ROC curves from the proposed discriminant models: PHWL and AHWL.

problematic." The development of new technology for data gathering would be very helpful and will be discussed later.

Table 10 lists the confusion matrices of all the tested discriminant models. It seems that the five-variable model PTHWL_Dis could be replaced by the four-variable model PHWL_Dis since the latter one has a better performance for characterizing the stability of landslide dams (with a higher percentage of landslide dams correctly classified). The performance of predictive models PHWL_Dis and AHWL_Dis are equivalently good.

The ROC plot is a convenient tool for decision-making in a risk management context (Begueria, 2006). Fig. 5 provides the ROC curves of the tested models. The performance of the proposed discriminant models PHWL_Dis (Eq. (4); $AUC = 93.5\%$) and AHWL_Dis (Eq. (6); $AUC = 90.5\%$) for predicting the stability of landslide dams is reasonably good. It should be noted that we did not further separate the 43 datasets into the subsets of earthquake-induced and heavy rainfall-induced landslide dams to construct the respective discriminant models due to insufficient data sets.

5.3. Discriminant models and DBI index-based graphic method

Korup (2004) concluded that the index-based graphic method is a promising, preliminary approach for the assessment of landslide-dam stability. Ermini and Casagli (2003) used a *DBI* index ($DBI < 2.75$ stable; $DBI > 3.08$ unstable) to classify 84 landslide dams (training set) with an overall prediction power of 75.0%. The rest of the 25% cases went unclassified ($2.75 < DBI < 3.08$).

To validate the index-based graphic approach, we use the DBI index proposed by Ermini and Casagli (2003) to classify 37 Japanese landslide dams (target set: 13 cases identical to those also in the worldwide dataset are removed). Only 64.9% of the 37 cases are correctly classified. The number of unclassified (or miss-classified) landslide dams increases to 35.1%. It is likely the low prediction rate of the *DBI* model is due to the fact that some dam volumes V_d are derived from the dam geometry, i.e., $V_d = 0.5 W_d L_d H_d$ (W_d = width; L_d = length; H_d = height) in Tabata's inventory. Therefore, the influence of dam height would be cancelled out in the *DBI* index.

We also use the worldwide dataset (84 landslide dams) (training set) to build AHV models with three variables (log-transformed catchment area LX_1, dam height LX_{11}, and dam volume LX_{16}). The discriminant model AHV_Dis is as follows:

$$D = -2.13LX_1 - 4.08LX_{11} + 2.94LX_{16} + 4.09 \quad (7)$$

The overall prediction power of the AHV_Dis is 88.1%, while the cross-validation accuracy is 83.3%. Using Eq. (7), the 37 Japanese landslide dams (target set), collected by Tabata et al. (2002), are classified into either stable or unstable landslide dams. The overall prediction power is 70.1% for model AHV_Dis. From this it can be seen that the discriminant models have a better performance than the index-based graphic approach does (overall prediction power is 64.9%).

We further use discriminant analysis to identify the significance of the three variables used. For the worldwide dataset, log-transformed dam volume is the most significant variable influencing the stability of a landslide dam ($SCDC = 1.759$). The remaining two variables, i.e., log-transformed dam height ($SCDC = -0.970$) and catchment area ($SCDC = -0.862$), have close importance and a negative influence on the stability of a dam. Notably, the correlation between log-transformed dam height and dam volume (0.730) is relatively high. Multi-colinearity problems may affect the variable-importance evaluation and the prediction ability of the derived discriminant models. Eq. (7) is only used solely for demonstrating the prediction performance between the discriminant models and the index-based graphic approach.

In summary, although the quality and accuracy of the proposed discriminant models are adequate within an order-of-magnitude scale, the problem of underreporting the landslide dam cases still somewhat exists, as stated by Korup (2004). It should be mentioned that the proposed statistical models must be used with caution. Recently, high resolution airborne LiDAR has been successfully utilized to evaluate the geomorphic characteristics of landslide processes (e.g. McKean and Roering, 2004; Chang et al., 2005; Chen et al., 2006). Developments in airborne LiDAR technologies, together with well developed GIS technologies, should permit the evaluation of the geomorphic characteristics of newly formed landslide dams and their stability in a more efficient, time-saving way and on a regional scale.

The development of new techniques for gathering the required information on the proposed models should greatly enhance the ability of the models to predict the stability of landslide dams. It is expected that records of landslide dams and complete geomorphic variables will be accumulated quickly after the new technique becomes more widely used. Additionally, increasing data availability and GIS-based geospatial extrapolation capability should expand the scope for future research to the formulation of regional susceptibility models for landslide-driven stream blockages based on these catchment parameters. The proposed discriminant models could serve as preliminary input for simulating the evolution of a landslide dam.

6. Conclusions

A method of rigorous discriminant analysis to quantitatively predict the stability of a landslide dam using relevant geomorphic variables has been presented herein. Based on 43 Japanese training cases, the log-transformed peak flows (or alternatively, the catchment area) are identified as the most significant geomorphic variables influencing the stability of a landslide dam. The log-transformed dam height, with a negative contribution to the stability of a landslide dam, is the second most significant variable. The log-transformed dam width and length have a similar positive effect on a dam's stability. Accordingly, the results provide a ranking of the relevant variables contributing to the stability of a landslide dam, which are not indicated in the current graphic approach adopted worldwide.

The good performance of the proposed discriminant models is indicated by the significant levels, overall success rate in the confusion matrices, and *AUC* of the ROC curves. The significance level of the PHWL model (log-transformed peak flow, dam height, dam width, and dam length) and the AHWL model (log-transformed catchment area, dam height, dam width, and dam length) is far less than 0.05. The *AUC* values of these two models are larger than 90%. More than 88.4% of landslide dams in the 43 training cases are correctly classified using the proposed four variable discriminant models. A high overall success rate for the cross-validation confirms the robustness of the proposed models when implemented to classify the stability of a landslide dam. It should be noted that the proposed discriminant models was built using a dataset of Japanese landslide dams only. The same multivariate statistical approach can be applied for an expanded dataset without any difficulty when more completely documented worldwide landslide-dam data is available. The implications of the present results for landslide dams elsewhere can be addressed in the future.

Finally, we have used the 84 cases of landslide dams (training dataset) reported by Ermini and Casagli (2003) to build a simplified three-variable (log-transformed catchment area, dam height, and dam volume) discriminant AHV model. Compared to the *DBI* model, where 64.9% of the Japanese cases were correctly classified, we have obtained a higher success rate for the AHV model, 70.1%, in its classification of 37 landslide dams, in spite of the possible multi-collinearity problem. In summary, the discriminant statistical model is promising to preliminarily assess the stability of landslide dams.

Acknowledgements

The work presented in this paper was made possible through the support of the Water Resources Planning Institute, Water Resources

Agency, Ministry of Economic Affairs, Taiwan, ROC. We thank the two anonymous reviewers and Editor for their very constructive comments which greatly improved the manuscript.

Appendix A. Supplementary data

Supplementary data associated with this article can be found, in the online version, at doi:10.1016/j.geomorph.2009.04.004.

References

Baeza, C., Corominas, J., 2001. Assessment of shallow landslide susceptibility by means of multivariate statistical techniques. Earth Surface Processes and Landforms 26, 1251–1263.
Begueria, S., 2006. Validation and evaluation of predictive models in hazard assessment and risk management. Natural Hazards 37, 315–329.
Carrara, A., Crosta, G., Frattini, P., 2008. Comparing models of debris-flow susceptibility in the alpine environment. Geomorphology 94, 353–378.
Casagli, N., Ermini, L., 1999. Geomorphic analysis of landslide dams in the Northern Apennine. Transactions of the Japanese Geomorphological Union 20, 219–249.
Casagli, N., Ermini, L., Rosati, G., 2003. Determining grain size distribution of material composing landslide dams in the Northern Apennine: sampling and processing methods. Engineering Geology 69, 83–97.
Chang, K.J., Taboada, A., Chan, Y.C., 2005. Geological and morphological study of the Jiufengershan landslide triggered by the Chi-Chi Taiwan earthquake. Geomorphology 71, 293–309.
Chang, K.T., Chiang, S.H., Lei, F., 2007. Analysing the relationship between typhoon-triggered landslides and critical rainfall conditions. Earth Surface Processes and Landforms 33, 1261–1271.
Chen, C.C., Tseng, C.Y., Dong, J.J., 2007. New entropy based method for variables selection and its application to the debris-flow hazard assessment. Engineering Geology 94, 19–26.
Chen, R.F., Chang, K.J., Angelier, J., Chan, Y.C., Deffontaines, B., Lee, C.T., Lin, M.L., 2006. Topographical changes revealed by high-resolution airborne LiDAR data: The 1999 Tsaoling landslide induced by the Chi-Chi earthquake. Engineering Geology 88, 160–172.
Chung, C.F., Fabbri, A.G., 2003. Validation of spatial prediction models for landslide hazard mapping. Natural Hazards 30, 451–472.
Clerici, A., Perego, S., 2000. Simulation of the Parma River blockage by the Corniglio landslide Northern Italy. Geomorphology 33, 1–23.
Costa, J.E., Schuster, R.L., 1988. The formation and failure of natural dam. Geological Society of America Bulletin 100, 1054–1068.
Costa, J.E., Schuster, R.L., 1991. Documented historical landslide dams from around the world. US Geological Survey Open File Report, pp. 91–239.
Cooley, W.W., Lohnes, P.R., 1971. Multivariate Data Analysis. John Wiley and Sons, New York.
Davis, J.C., 2002. Statistics and Data Analysis in Geology, (3rd Ed.). John Wiley and Sons, New York.
Dillon, W.R., Goldstein, M., 1986. Multivariate Analysis: Methods and Applications. John Wiley and Sons, New York.
Ermini, L., Casagli, N., 2003. Prediction of the behaviour of landslide dams using a geomorphological dimensionless index. Earth Surface Processes and Landforms 28, 31–47.
Klecka, W.R., 1980. Discriminant analysis. Sage University Paper series on Quantitative Applications in the Social Sciences. Sage Publications, Beverly Hills and London, pp. 07–019.
Korup, O., 2002. Recent research on landslide dams — a literature review with special attention to New Zealand. Progress in Physical Geography 26, 206–235.
Korup, O., 2004. Geomorphometric characteristics of New Zealand landslide dams. Engineering Geology 73, 13–35.
Korup, O., 2005. Geomorphic hazard assessment of landslide dams in South Westland, New Zealand: fundamental problems and approaches. Geomorphology 66, 167–188.
Lee, C.T., Huang, C.C., Lee, J.F., Pan, K.L., Lin, M.L., Dong, J.J., 2008a. Statistical approach to earthquake-induced landslide susceptibility. Engineering Geology 100, 43–58.
Lee, C.T., Huang, C.C., Lee, J.F., Pan, K.L., Lin, M.L., Dong, J.J., 2008b. Statistical approach to storm event-induced landslides susceptibility. Natural Hazards and Earth System Sciences 8, 941–960.
McCuen, R.H., 1998. Hydrologic Analysis and Design. Prentice Hall.
McKean, J., Roering, J., 2004. Objective landslide detection and surface morphology mapping using high-resolution airborne laser altimetry. Geomorphology 57, 331–351.
Schuster, R.L., Costa, J.E., 1986. A perspective on landslide dams. In: Schuster, R.L. (Ed.), Landslide Dam: Processes Risk and Mitigation. American Society of Civil Engineers. Geotechnical Special Publication, vol. 3, pp. 1–20.
Swanson, F.J., Oyagi, N., Tominaga, M., 1986. Landslide dam in Japan. In: Schuster, R.L. (Ed.), Landslide Dam: Processes Risk and Mitigation. American Society of Civil Engineers. Geotechnical Special Publication, vol. 3, pp. 131–145.
Swets, J.A., 1988. Measuring the accuracy of diagnostic systems. Science 204 (4857), 1285–1293.
Tabata, S., Mizuyama, T., Inoue, K., 2002. Natural Landslide Dams Hazards. Kokonshoin, Tokyo. (in Japanese).